41. K. J. Keeler and G. B. Gloor, *Mol. Cell. Biol.* **17**, 627 (1997)
42. Y. Bellaiche, V. Mogila, N. Perrimon, *Genetics* **152**, 1037 (1999).
43. We thank M. Golic and S. Titen for technical as-

Negative Poisson's Ratios for Extreme States of Matter

Ray H. Baughman,[1]* Socrates O. Dantas,[2] Sven Stafström,[3] Anvar A. Zakhidov,[1] Travis B. Mitchell,[4] Daniel H. E. Dubin[5]

Negative Poisson's ratios are predicted for body-centered-cubic phases that likely exist in white dwarf cores and neutron star outer crusts, as well as those found for vacuumlike ion crystals, plasma dust crystals, and colloidal crystals (including certain virus crystals). The existence of this counterintuitive property, which means that a material laterally expands when stretched, is experimentally demonstrated for very low density crystals of trapped ions. At very high densities, the large predicted negative and positive Poisson's ratios might be important for understanding the asteroseismology of neutron stars and white dwarfs and the effect of stellar stresses on nuclear reaction rates. Giant Poisson's ratios are both predicted and observed for highly strained coulombic photonic crystals, suggesting possible applications of large, tunable Poisson's ratios for photonic crystal devices.

Rubber bands, Jell-O, and soft biological tissues share an important and unusual property with ultradense crystals in neutron stars and white dwarfs (1–3), vacuumlike ion crystals in electromagnetic traps (4–6), and crystallized colloids (7–16). Each can behave as if they are incompressible when stretched. This means that the fractional volume change, $\Delta V/V$, produced by a fractional elongation, $\Delta L/L$, is so small that the derivative $\gamma \equiv (L/V)(dV/dL)$ approaches zero. This behavior is described with the Poisson's ratio, which is defined as $\nu_{ij} = -\varepsilon_j/\varepsilon_i$, where ε_j is the lateral strain in the j-axis direction arising from a strain of ε_i applied in a longitudinal i-axis direction. The sum of Poisson's ratios for a stretch direction must approach unity for an effectively incompressible solid. Hence, isotropic rubbers and soft tissues have Poisson's ratios of ~0.5 (17, 18).

In contrast, negative Poisson's ratios are known for reentrant foams and related structures (17–19), microporous polymers (20), polymer laminates (21), hinged phases (22, 23), the noncubic phases of arsenic, bismuth, and α-cristobalite (24, 25), and certain cubic metals (26, 27). These materials have the counterintui-

tive property of expanding laterally when stretched, but none behaves as incompressible when stretched. For example, the sum of Poisson's ratios is between 1.15 and 1.59 for the cubic metallic elements (27), so they provide large values of $(L/V)(dV/dL)$.

Here, we investigate whether effectively incompressible crystal phases of white dwarf stars, neutron stars, and colloids can have negative Poisson's ratios. The search for materials with negative Poisson's ratios has focused on materials with large bending or torsional interactions and a large ratio of shear modulus to bulk modulus (17, 18), which are on the opposite extreme from these unusual states of matter with two-body, central-force interactions and a small ratio of shear modulus to bulk modulus. We predict the effects of coulombic screening, stretch-induced density changes, temperature, large crystal strains, and ion mixing on the extremal Poisson's ratios. Finally, we obtain experimental evidence of negative Poisson's ratios for one of these unusual states of matter.

The minimum and maximum Poisson's ratios for cubic crystals are usually for a stretch along a [110] direction, which is a cube-face diagonal, and resulting lateral deformations measured along the orthogonal [1$\bar{1}$0] and [001] directions, respectively. These Poisson's ratios can be expressed as functions of the Poisson's ratio, ν_{12}, and the tensile and shear elastic compliances, S_{11} and S_{44}, for the cube-axis directions (27):

$$\nu(1\bar{1}0) = -[1 - \nu_{12} - (S_{44}/2S_{11})]/[1 - \nu_{12} + (S_{44}/2S_{11})] \quad (1)$$

and

$$\nu(001) = 2\nu_{12}/[1 - \nu_{12} + (S_{44}/2S_{11})] \quad (2)$$

We use these equations to predict the allowable range of $\nu(1\bar{1}0)$ and $\nu(001)$ for a cubic crystal that behaves as incompressible when stretched. Stability requires that S_{11} and S_{44} are both positive. Substituting $\nu_{12} = 0.5$ into Eqs. 1 and 2 shows (Fig. 1A) that $1 \geq \nu(1\bar{1}0) \geq -1$, $2 \geq \nu(001) \geq 0$, and $\nu(1\bar{1}0) < 0$ when $S_{44}/S_{11} < 1$, which corresponds to high elastic anisotropy. A negative Poisson's ratio means that stretching causes a lateral expansion, which contradicts common experience for ordinary materials that act incompressible—like rubber bands.

Star crystals: Effectively incompressible crystals with unscreened charges. White dwarf cores and the outer crusts of neutron stars have been long proposed to consist of ultradense metallic crystals (1–3). These body-centered-cubic (bcc) crystals would have Fermi energies and electron densities that can be orders of magnitude higher than those of conventional metals. One might expect only positive Poisson's ratios for ultradense crystals, because the minimum Poisson's ratios of ordinary bcc metals become positive when the Fermi energy and electron density are large. The difference in bonding explains why this result for conventional metals is not valid for ultradense metals, as well as why ultradense metals behave as incompressible when stretched. The structure of an ordinary bcc metal can be approximated as arising from the balance between an attractive interaction between atom cores and the repulsive volume-dependent electron gas energy (28). At high pressures the atom cores shrink by loss of electrons to the electron gas. Eventually, at ultrahigh pressures the solid consists of well-separated nuclei in a free-electron sea. The electrostatic interactions between nuclei then dominate crystal shape, and the opposing contributions from the Fermi energy and pressure determine the crystal volume. Any significant volume change would enormously increase the energy change required for elongation, and tensile elongations therefore proceed at essentially constant volume. Hence, ultradense matter behaves like an anisotropic type of Jell-O (29), elongating and shearing much more readily than changing volume. These arguments pertain for densities between ~10^4 g/cm^3 and ~10^{11} g/cm^3, which are much lower than nuclear densities (~2×10^{14} g/cm^3). Outside this range, either the atom cores are incompletely ionized (when density and pressure are too

[1]Honeywell International, Honeywell Technology Center, Morristown, NJ 07962–1021, USA. [2]Departamento de Física, Universidade Federal de Juiz de Fora (UFJF), Juiz de Fora, 36036-330, Mina Gerais, Brazil. [3]Department of Physics and Measurement Technology, Linköping University, S-581 83, Linköping, Sweden. [4]National Institute of Standards and Technology, Boulder, CO 80303, USA. [5]Department of Physics, University of California at San Diego, La Jolla, CA 92093, USA.

*To whom correspondence should be addressed. E-mail: ray.baughman@honeywell.com

low), or the nuclei are in too close proximity (when density and pressure are too high) for short-range interactions and many-body forces to be ignored.

So that derived results extend from ultradense matter to other types of coulombic crystals, Poisson's ratios were calculated as a function of screening parameter λ for a Yukawa phase. This is a phase whose interparticle interactions are described by the Yukawa potential, $r^{-1} \exp(-\lambda r/a_{WS})$, where a_{WS} is the Wigner-Seitz radius (the radius of a sphere having the volume of a particle in the crystal) and r is the interion separation. The extremal Poisson's ratios were derived by elongating the crystal in the [110] direction and varying other crystal dimensions to minimize electrostatic energy, while maintaining the initial volume. These Poisson's ratios were directly obtained from axial strains by representing the cubic structure by a face-centered tetragonal cell, whose axes are a cubic axis and two face diagonals for the bcc cell. Calculations for crystallized layers of ions having finite crystal thicknesses were similar, except that variations in the interlayer separation within ion crystal stacks were permitted.

The screening parameter λ vanishes for the ultradense matter in white dwarfs and neutron stars, because electronic charge is uniformly distributed (as a result of giant electron Fermi energies). The calculated extremal Poisson's ratios for the bcc structure are then $\nu(1\bar{1}0) = -0.426$ and $\nu(001) = 1.426$ (Fig. 1B). Despite the 10^{11} times higher possible density and the very different nature of interactions, the calculated minimum Poisson's ratios [$\nu(1\bar{1}0)$] for the ultradense matter and those from experiments on alkali metals (27) are surprisingly similar (−0.43 for Li, −0.44 for Na, −0.46 for K, −0.40 for Rb, and −0.36 for Cs).

Colloidal crystals: Effectively incompressible crystals with screened charges. Colloidal crystals consisting of well-separated, spherical colloidal particles in a liquid matrix (7–13) provide the opposite extreme from ultradense matter, because partial screening by a nonuniform distribution of ions causes λ to be nonzero. We assume a usual case where repulsive intersphere interactions cause the crystal to fill the available fluid volume. As for ultradense matter, these colloidal crystals are well approximated as being incompressible (because it costs much less energy to change crystal shape than to change crystal volume). Screening makes $\nu(1\bar{1}0)$ more negative and $\nu(001)$ more positive until the limiting values of $\nu(1\bar{1}0) = -1$ and $\nu(001) = 2$ are reached (where the bcc phase is not mechanically stable) (Fig. 1B). This trend for $\nu(1\bar{1}0)$ to become more nega-

tive as the decay of repulsive potential increases is generally valid for incompressible bcc crystals with repulsive interparticle interactions. Body-centered-cubic crystals have lower energies than face-centered-cubic (fcc) crystals with the same density only for λ below 1.066, and thus the minimum Poisson's ratio lies in a much more restricted range (between −0.461 and −0.426, from Fig. 1B) for a globally stable, incompressible bcc crystal based on the Yukawa potential.

Known limitations of the Yukawa potential for representing interactions in colloidal crystals (14, 15) do not change the conclusion that $\nu(1\bar{1}0)$ is negative for the bcc phase. Specifically, the Sogami potential (14) is widely used to decrease these limitations (by adding an attractive interaction), and we find that this potential provides precisely the same range for $\nu(1\bar{1}0)$ for a bcc phase as does the Yukawa potential (−1 to −0.426). Independent of the specific two-body interaction po-
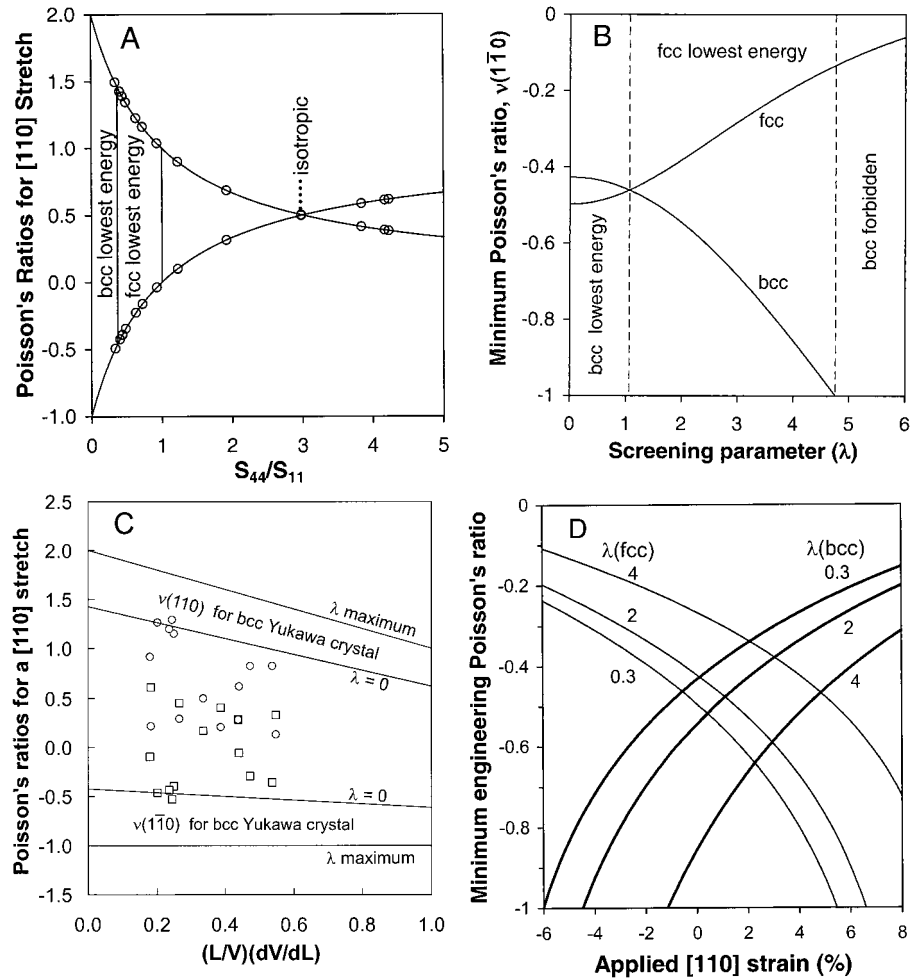
Fig. 1. Poisson's ratios calculated for diverse types of screened and unscreened coulombic crystals. (**A**) The dependence of $\nu(001)$ and $\nu(1\bar{1}0)$ (top and bottom curves) upon the ratio of shear compliance to tensile compliance (S_{44}/S_{11}) for a cubic solid that behaves as incompressible when stretched. The labeled parameter ranges indicate where the most stable Yukawa phase is either bcc or fcc. The unlabeled parameter ranges are inaccessible for either of these coulombic phases. The open circles on the curves are the constant-volume Poisson's ratios for the bcc metals, calculated (with Eq. 3) from the experimentally derived Poisson's ratios (27). (**B**) The dependence of $\nu(1\bar{1}0)$ on the coulomb screening parameter λ for Yukawa bcc and fcc phases. The vertical dashed lines indicate the ranges of λ where (at the same density) either bcc or fcc is more stable, as well as where a bcc phase does not have an energy minimum. (**C**) The dependence of $\nu(1\bar{1}0)$ and $\nu(001)$ on (L/V)(dV/dL), calculated by applying Eq. 3 to the results of Fig. 1B. These results for a bcc phase are valid for values of λ in the Yukawa potential that result in at least mechanical stability and any functional form for the volume dependence of total energy. The top pair of curves is for $\nu(001)$, and the bottom pair is for $\nu(1\bar{1}0)$. The region between the curves in each pair (labeled according to the screening parameter λ) indicates the restricted parameter range allowed for a stable bcc phase. The observed Poisson's ratios (27) as a function of (L/V)(dV/dL) for bcc metals [○ and □ for $\nu(001)$ and $\nu(1\bar{1}0)$, respectively] have little overlap with the allowed range for Yukawa bcc crystals. (**D**) The minimum engineering Poisson's ratio versus the applied [110] strain for incompressible Yukawa bcc and fcc crystals having the indicated λ. The minimum engineering Poisson's ratio is the negative ratio of the finite strain in the [1$\bar{1}$0] direction to the finite applied [110] strain.

tential, $v(1\bar{1}0)$ approaches -1 as the bcc phase disappears as an energy minimum because the elastic constant difference $C_{11} - C_{12}$ goes to zero (which is the case for a bcc rigid-sphere crystal).

Body-centered-cubic arrangements of virus particles provide special types of colloidal crystals, which can also provide negative Poisson's ratios. One possible example is the approximately spherical ($\sim$330 Å diameter) tomato bushy stunt virus, which consists of 180 copies of a protein arranged on an icosohedral surface surrounding a single piece of RNA (30). At appropriately low concentrations in a suitable solution, charged virus particles fill the available fluid volume with a bcc arrangement of separated particles, and the above-calculated Poisson's ratios for a repulsive coulombic potential should thus describe the elastic behavior. The minimum Poisson's ratio is also expected to be negative in the opposite extreme of very high particle densities (where the virus particles are in contact, or separated only by solvating molecules), as long as the phase is bcc and the effects of many-body and noncentral forces can be approximated by an effective pairwise interaction potential between particle centers. The point is that a bcc phase having only nearest-neighbor, central-force interactions is mechanically unstable to shear [because $v(1\bar{1}0) = -1$]. If many-body, noncentral force or long-range interactions are just barely sufficient to stabilize the bcc phase, the minimum and maximum Poisson's ratios will be close to -1 and 2, respectively.

Ion crystals: Crystals with controllable compressibility and no screening. The stretch-induced volume change of laser-cooled ion crystals depends on the process providing crystal elongation. These crystals, called sparse crystals because they have the density of a good vacuum, consist of crystallographic arrays of individual ions (4–6). Because there is no counter charge, ion confinement must be provided by the field of an electromagnetic trap, which has the same effect as a uniform background charge with equal density to that of the ion array but opposite sign. Such ion plasmas having three-dimensional extension can crystallize into a bcc lattice when $\Gamma \equiv (Ze)^2/(a_{WS}kT) > \sim 170$, where Z is the number of electron charges e per particle, a_{WS} is the Wigner-Seitz radius, k is Boltzmann's constant, and T is absolute temperature (4–6). When enough ions are in the trap, well-ordered bcc crystals (with interion distances of about 10 μm) form at low temperatures ($\approx$10 mK). Like ferroelectrics, where the Poisson's ratio depends on whether deformation is at constant field or constant polarization, the Poisson's ratio for sparse crystals depends on the nature of the elongation process, which is accomplished by varying the electrical and magnetic fields of the

electromagnetic trap. If the electromagnetic field is varied to provide deformation at constant counter-charge density (such as by varying only the axial electric potential for a Penning trap), the constant-volume Poisson's ratios result for an ion array that is effectively infinite in three dimensions [$v(1\bar{1}0) = -0.426$ and $v(001) = 1.426$]. The Poisson's ratios $v_{ij}(\gamma)$ for other combinations of electric and magnetic field changes that produce a nonzero value of $\gamma \equiv (L/V)(dV/dL)$ are related to the constant-volume Poisson's ratios $v_{ij}(0)$ by

$$v_{ij}(\gamma) = v_{ij}(0) - (\gamma/3)[v_{ij}(0) + 1] \quad (3)$$

This equation is easily derived by recognizing that $v_{ij}(\gamma)$ results from the superposition of isotropic strains on the anisotropic strains resulting from $v_{ij}(0)$. Interestingly, $v(1\bar{1}0)$ only changes from -0.426 to -0.618 as γ goes from zero to unity.

Plasma dust crystals: Crystals with controllable compressibility and screening. Body-centered-cubic plasma dust crystals can have both large λ and large stretch-induced volume changes. Such crystals (consisting of micrometer-sized, highly charged dust particles in a plasma having compensating charge density) are easily created in the laboratory and are possible components of planetary rings, comets, and highly luminescent clouds seen in Earth's upper atmosphere (31–33). As for sparse crystals, the Poisson's ratios depend on experimental conditions during crystal deformation. However, the force field is generally complicated for dust plasma crystals (reflecting coulomb repulsion, sheath field, gravity, and ion drag effects), and a Yukawa potential is useful only when the plasma flow velocity (relative to the dust particles) is much smaller than the ion thermal velocity. Use of a nonzero λ then corrects for the screening of particle charge by the plasma electrons and ions (31–33). The dependence of $v(1\bar{1}0)$ on γ is very small for all values of the screening coefficient λ (Fig. 1C). In fact, we predict that $v(1\bar{1}0)$ will be negative for the most physically reasonable values of γ (between -2.2 and infinity) and a λ that is compatible with a stable bcc lattice. Also, the predicted $v(1\bar{1}0)$ becomes increasingly negative during the constant-volume compression of a bcc coulombic crystal in the [110] direction (Fig. 1D).

Effects of bcc-to-fcc transition and ion mixing. A fcc phase with only nearest-neighbor central-force interactions does not have a negative Poisson's ratio [$v(1\bar{1}0) = 0$ and $v(001) = 1/2$], whereas the corresponding bcc phase has a highly negative Poisson's ratio [$v(1\bar{1}0) = -1$ and $v(001) = 2$] (27). We therefore investigated whether negative Poisson's ratios arise for fcc coulombic crystals. Figure 1B shows that a Yukawa fcc crystal (such as a colloidal crystal) provides a nega-

tive $v(1\bar{1}0)$. With increasing λ, this Poisson's ratio increases from -0.497 to 0. Interestingly, $v(1\bar{1}0)$ for bcc is less negative than for fcc until the energy of the fcc phase becomes lower than that of bcc. Simultaneous transitions in relative energy and relative Poisson's ratios occur at a screening length of $\lambda = 1.066$, corresponding to $v(1\bar{1}0) = -0.461$. We also obtain this simultaneous switching in relative energy and Poisson's ratio [again at $v(1\bar{1}0) = -0.461$] when the particle size is negligible and the Yukawa potential is replaced by the Sogami potential (14). The results in Fig. 1, B and D, show that fcc and bcc phases provide oppositely directed dependencies of $v(1\bar{1}0)$ on both screening parameter and [110] strain.

The effect on Poisson's ratio of forming a binary phase with two ions having a charge ratio R_z is also interesting, especially because the degree of chemical separation in the interiors of white dwarf stars is not well established. At low temperatures, Ogata et al. (34) predict that dense binary compositions form CsCl-type crystals (together with pure bcc crystals of the excess component) for R_z below about 2.3, and pure bcc crystals of each species for higher R_z up to 5.0 (the calculation limit). The CsCl structure is bcc-like, but with different ions on the body center than on the cell corners. Our static-lattice calculations for the CsCl lattice (Fig. 2) show that $v(1\bar{1}0)$ becomes positive when R_z exceeds 1.56. However, the calculated $v(1\bar{1}0)$ is still negative (-0.22) for a CsCl-type plasma crystal composed of carbon and oxygen ions ($R_z = 4/3$), which is believed (34) to be the main component left from helium burning for most white dwarfs. Monte Carlo calculations at high temperature (34) predict nearly complete chemical separation upon solidification for R_z above about 1.6. The average $v(1\bar{1}0)$ should therefore return to the single-ion lattice result for R_z above this value. Negative Poisson's ratios are also expected as a result of phase separation for more complex total-ion concentrations. For example, phase separation is predicted (34) to produce solid Ne cores from ^{12}C-^{16}O-^{22}Ne mixtures in white dwarf interiors, even though Ne is only a trace component.

Temperature dependence. We have so far ignored temperature effects on Poisson's ratio. Simple arguments suggest that the temperature dependence will be small, unless temperature changes the fundamental nature of bonding (as in the conversion of ion cores to fully ionized nuclei for ultradense matter) or the degree of coulombic screening. Because smearing the particle-centered charge over spheres about the mean particle centers does not change the effective distance dependence of interparticle potential, the zero-order effect of temperature on Poisson's ratio vanishes. This agrees with results we derive
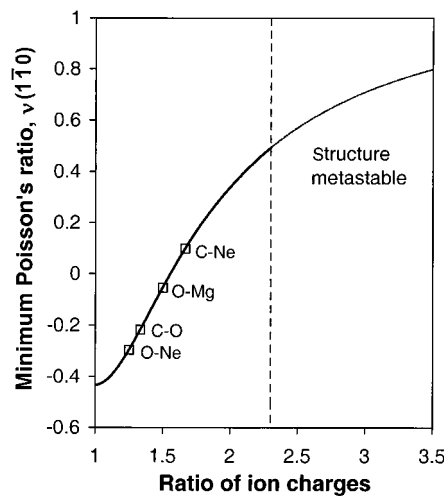
from the measured temperature dependence of elastic compliances (*35*) for the alkali metals. For example, $\nu(1\bar{1}0)$ for potassium increases only from -0.49 to -0.40 in going from near 0°K to the melting point [whereas $\nu(001)$ decreases from 1.22 to 1.20]. The same conclusion results if we use Eq. 1 to derive the temperature dependence of $\nu(1\bar{1}0)$ for an incompressible phase from elastic shear moduli calculated by the Monte Carlo method (*36, 37*) for a bcc coulombic crystal having unscreened charges. The calculated minimum Poisson's ratio changes only from -0.426 for $\Gamma = \infty$ ($T = 0$) to -0.36 for $\Gamma = 200$ (near the melting point).

Experimental evidence. Observed lateral-dimension changes of crystallized ion plasmas as a function of axial length provide experimental evidence that bcc coulombic crystals with vacuumlike density (10^{-15} g/cm³) have a negative Poisson's ratio over a wide range of applied strains. Images of laser-cooled arrays of $^9Be^+$ ions confined in a Penning trap at $T < 10$ mK were simultaneously recorded for orthogonal directions, as previously described (*6*). In contrast to previous experiments, the deformations of the trapped ion arrays were made at nearly constant volume (by varying only the axial electric potential), which is the deformation mode for analogous Wigner crystals in neutron and white dwarf stars. The investigated arrays consist of ion layers that are stacked so that the [110] direction coincides with the magnetic field direction. The effect of a [110] strain on the orthogonal [1$\bar{1}$0] strain (Fig. 3) was obtained from measurements of the length of the primitive intralayer interion vector, the intralayer angle between equivalent vectors, and the average separation between layers for a four-layer stack. The interlayer separation increases as the interlayer repulsion decreases with decreasing number of layers (Fig. 3). Both the theoretical and experimental results of Fig. 3 show that an increase in the [110] distance increases the orthogonal [1$\bar{1}$0] distance, demonstrating that $\nu(1\bar{1}0)$ is negative for the wide range of applied [110] strains. While the minimum and maximum Poisson's ratio for an undeformed cubic phase cannot exceed in magnitude -1 and 2, respectively, the theoretical curve for the four-layer structure provides $\nu(1\bar{1}0) = -3.1$ and $\nu(1\bar{1}0) = 4.1$ at close to the maximum observed compression in the [110] direction. These values are about an order of magnitude larger than typical Poisson's ratios for crystals. Such extreme Poisson's ratios partially reflect the 13% range of strains in [110] axis dimension that is experimentally accessible for the four-layer ion crystal before either plastic deformation or a phase transition occurs (to either observed fcc or hexagonal phases).

**Discussion.** The ability to adjust Poisson's

ratios to desired values is potentially useful for employing colloidal crystals, sparse crystals, and dusty plasma crystals as gratings for mechanically or electromechanically controlled diffraction (as in narrow-band rejection filters, nanosecond optical switches, and sensors) or lasing (*13*). Such application possibilities exist because these materials are photonic crystals at typically optical, infrared, and microwave wavelengths, respectively—meaning that they have lattice periodicities sufficient to diffract and confine electromagnetic radiation at these wavelengths. When the Poisson's ratios are tuned to extremal values for undistorted cubic phases [approaching $\nu(1\bar{1}0) = -1$ and $\nu(001) = 2$ for an undistorted cubic phase], an applied strain in the [110] direction can be amplified nearly twofold in [001] strain, and the difference between [1$\bar{1}$0] and [001] strains can approach three times the applied strain. This might be useful for sensor applications and the control of light propagation and emission within photonic band gaps. Also, we find (Fig. 3) that this amplification of strain and strain difference can be increased to factors of over 4.1 and 7.2, respectively, by using the giant Poisson's ratios obtainable for highly strained bcc coulombic phases. Moreover, our results show that the Poisson's ratios can be finely tuned by varying the screening parameter λ (such as by changing the salt concentration or particle density of a colloidal crystal), the volume change during deformation, or the initial lattice strain, or by introducing particles having different charges.

It is remarkable that negative Poisson's ratios, a property once considered rare, can be expected from coulomb interactions over such a broad range of densities—from less

than 10^{-15} g/cm³ for sparse-matter crystals to at least 10^{11} g/cm³ for ultradense matter (unit cell parameters from about 10^{-3} Å for ultradense matter to millimeters for dusty plasma crystals). Also, we predict nearly the same negative Poisson's ratios over an enormous temperature range, from above 10^6 K for ultradense white dwarfs and neutron star crystals to 0 K for the constant-volume deformation of sparse crystals. If the cores of white dwarfs and the outer crusts of neutron stars are really crystalline, as has been long suspected, crystals with negative Poisson's ratios would be a common crystalline state of matter in the universe. The predicted extremal Poisson's ratios for these ultradense states of matter might be important for understanding the effect of anisotropic stellar stresses on nuclear reaction rates in the inner crusts of neutron stars (*38*), as well as the asteroseismology of white dwarf stars and neutron star quakes, which are being characterized by interpreting radiation pulses from the stars (*3*).
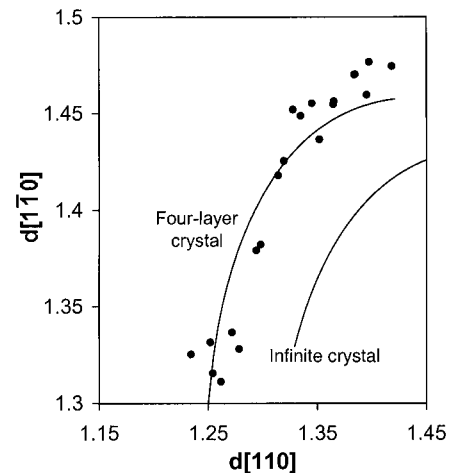
Fig. 3. The experimentally derived and calculated relation between the crystal dimensions in the [1$\bar{1}$0] and [110] directions (d[1$\bar{1}$0] and d[110]) during the elongation of a bcc sparse crystal in the [110] direction without change in volume. These dimensions are normalized to provide a volume of 0.5 per ion, so d[1$\bar{1}$0] and d[110] are $2^{1/2}$ for an unstrained three-dimensionally infinite crystal. The experimentally determined results (●) are for a four-layer stack of $^9Be^+$ ions in a Penning trap, which is highly extended in two in-plane directions, [1$\bar{1}$0] and [001]. The solid curves are theoretical predictions for a four-layer ion crystal and for a three-dimensionally infinite ion crystal. Both the experimental and theoretical results provide negative Poisson's ratios for the [1$\bar{1}$0] direction over a wide range of strains, because d[1$\bar{1}$0] increases with increasing elongation of d[110]. The high slope of the dependencies evident at small values of d[110] correspond to giant negative Poisson's ratios, as well as giant positive Poisson's ratios (because the sum of Poisson's ratios for orthogonal directions is unity for solids that behave as incompressible).

Fig. 2. The calculated dependence of $\nu(1\bar{1}0)$ on the ratio of ion charges for a structure that is derived from a bcc lattice by changing the magnitude of the charges at the body-center sites relative to those on the cell corners. The indicated chemical compositions (□) are those relevant for white dwarf stars.

References and Notes
1. H. M. Van Horn, *Science* **252**, 384 (1991).
2. G. Baym and D. Pines, *Ann. Phys.* **66**, 816 (1971).
3. D. E. Winget, *J. Phys. Condens. Matter* **10**, 11247 (1998).
4. W. M. Itano *et al.*, *Science* **279**, 686 (1998).
5. J. Schiffer, *Science* **279**, 675 (1998).
6. T. B. Mitchell *et al.*, *Science* **282**, 1290 (1998).
7. D. Hone, S. Alexander, P. M. Chaikin, P. Pincus, *J. Chem. Phys.* **79**, 1474 (1983).
8. W. Shih, I. A. Aksay, R. Kikuchi, *J. Chem. Phys.* **86**, 5127 (1987).
9. R. S. Crandall and R. Williams, *Science* **198**, 293 (1977).
10. N. A. Clark, A. J. Hurd, B. J. Ackerson, *Nature* **281**, 57 (1979).
11. C. Murray and D. G. Grier, *Annu. Rev. Phys. Chem.* **47**, 421 (1996).
12. A. van Blaaderen and P. Wiltzius, *Adv. Mater.* **9**, 833 (1997).
13. J. M. Weissman, H. B. Sunkara, A. S. Tse, S. A. Asher, *Science* **274**, 959 (1996).
14. J. Yamanaka, H. Yoshida, T. Koga, N. Ise, T. Hashimoto, *Phys. Rev. Lett.* **80**, 5806 (1998).
15. A. E. Larsen and D. G. Grier, *Nature* **385**, 230 (1997).
16. M. O. Robbins, K. Kremer, G. S. Grest, *J. Chem. Phys.* **88**, 3286 (1988).
17. R. S. Lakes, *Science* **235**, 1038 (1987).
18. ———, *J. Mater. Sci.* **26**, 2287 (1991).
19. L. J. Gibson, M. F. Ashby, G. S. Schajer, C. I. Robertson, *Proc. R. Soc. London Ser. A* **382**, 25 (1982).
20. K. E. Evans, M. A. Nkansah, I. J. Hutchinson, S. C. Rogers, *Nature* **353**, 124 (1991).
21. G. W. Milton, *J. Mech. Phys. Solids* **40**, 1105 (1992).
22. R. H. Baughman and D. S. Galvão, *Nature* **365**, 735 (1993).
23. R. H. Baughman, S. Stafström, C. Cui, S. O. Dantas, *Science* **279**, 1522 (1998).
24. A. Yeganeh-Haeri, D. J. Weidner, J. B. Parise, *Science* **257**, 650 (1992).
25. D. J. Gunton and G. A. Saunders, *J. Mater. Sci.* **7**, 1061 (1972).
26. F. Milstein and K. Huang, *Phys. Rev.* **19**, 2030 (1979).
27. R. H. Baughman, J. M. Shacklette, A. A. Zakhidov, S. Stafström, *Nature* **392**, 362 (1998).
28. J. M. Thomas, *Scr. Metall.* **5**, 787 (1971).
29. M. A. Rudman, *Sci. Am.* **224**, 24 (February 1971).
30. P. A. Timmins, *Makromol. Chem. Macromol. Symp.* **15**, 311 (1988).
31. J. H. Chu and I. Lin, *Phys. Rev. Lett.* **72**, 4009 (1994).
32. M. Rosenberg and G. Kalman, *Phys. Rev. E* **56**, 7166 (1997).
33. J. B. Piper, J. Goree, R. A. Quinn, *Phys. Rev. E* **54**, 5636 (1996).
34. S. Ogata, H. Iyetomi, S. Ichimaru, H. M. Van Horn, *Phys. Rev. E* **48**, 1344 (1993).
35. A. G. Every and A. K. McCurdy, in *Landolt-Börnstein*, D. E. Nelson, Ed. (New Series III/29a, Springer, Berlin, 1992), pp. 11–43.
36. S. Ogata and S. Ichimaru, *Phys. Rev. A* **8**, 4867 (1990).
37. The shear elastic moduli $C_{11} - C_{12}$ and C_{44} are reported as a function of Γ in (*36*). We calculate $\nu(1\bar{1}0)$ from these moduli using Eq. 1 and our derived relation $S_{44}/2S_{11} = 3/4\,[(C_{11} - C_{12})/C_{44}]$ for cubic crystals having an axial Poisson's ratio of 0.5.
38. From the predicted Poisson's ratios at low temperature and at close to the melting point, the effect of a [110] strain on the separation between reacting nuclei is 2.61 times and 2.34 times smaller at these respective temperatures than for an isotropic crystal that behaves as incompressible.
39. We thank J. J. Bollinger, M. C. Robbins, and J. R. Knox for helpful discussions. Partially supported by Defense Advanced Research Project Agency grant DAAB07-97-C-J036 and a New Energy Development Organization grant on "Tunable Photonic Crystals." S.O.D. thanks the Brazilian agency CAPES for financial support as a visiting scholar.

27 January 2000; accepted 2 May 2000

R E P O R T S

Viscosity Mechanisms in Accretion Disks

Kristen Menou

The self-sustained turbulence that develops in magnetized accretion disks is suppressed in the weakly ionized, quiescent disks of close binary stars. Because accretion still proceeds during quiescence, another viscosity mechanism operates in these systems. An anticorrelation of the recurrence times of SU UMa dwarf novae with their mass ratio supports spiral waves or shockwaves tidally induced by the companion star as the main process responsible for accretion in the quiescent disks. Other weakly ionized gaseous disks in systems lacking a massive companion must rely on yet another transport mechanism, or they could be essentially passive.

Accretion discs (*1*) are present in a variety of astrophysical objects, such as mass-transfer binaries, young stellar systems, and active galactic nuclei (*2*). The main uncertainty about the structure of accretion disks is the nature and magnitude of their viscosity (*3*), the process by which the gas loses angular momentum to accrete onto the massive central object. Theoretical studies of magnetized accretion disks have shown that magnetohydrodynamical (MHD) turbulence provides the necessary outward angular momentum transport for accretion to proceed (*4, 5*). The problem of identifying a viscosity mechanism can also be addressed empirically by constraining the magnitude of viscosity in unsteady disks, where it directly relates to the observed variability (*2*). This is best done in transient close binaries, such as recurrent

Department of Astrophysical Sciences, Princeton University, Princeton, NJ 08544, USA.

dwarf novae, with geometries, masses, and mass accretion rates that are relatively well known (*6*).

The transient nature of accretion in the disks of close binaries is understood as a thermal-viscous limit cycle because of sudden changes of the disk opacity when hydrogen recombines (*7*). Global disk evolution models reproduce the main properties of observed outbursts, but only if the efficiency of transport and dissipation is less in quiescence than during outburst (*8, 9*). This requirement is consistent with the low level of ionization predicted in quiescence. In terms of the magnetic Reynolds number

$$Re_{\mathrm{M}} \equiv C_{\mathrm{s}}H/\eta \qquad (1)$$

where C_{s} is the sound speed, H is the disk scale height, and η is the resistivity (inversely proportional to the ionization fraction), local shearing-box MHD simulations (*10, 11*) predict a reduced efficiency of angular momen-

tum transport when $Re_{\mathrm{M}} \lesssim 10^4$, a value comparable to what is expected in quiescent disks (*12*). It is unclear, however, whether MHD turbulence is still responsible for transport during this phase (at a reduced level) or is entirely suppressed.

This question is addressed here by using results from shearing-box simulations as input for a global numerical model designed to study disk instabilities (*13*). The model provides reliable values for the temperature, density, and therefore Re_{M}, throughout the disk [thermal ionization and resistive diffusion are the dominant processes in the disks considered here (*12*)]. The viscosity parameter α used in the model (a measure of the disk viscosity in units of $C_{\mathrm{s}}H$) is tabulated as a function of Re_{M} according to the most recent (zero net flux) MHD simulations that include resistive effects (*11*). The decay of α is locally limited to an e-folding time scale, corresponding to four orbits, to allow for the finite time of field resistive diffusion. Other model parameters are chosen to represent the disk around the white dwarf of the prototypical dwarf nova SS Cyg (*12*): mass of the primary $M_1 = 1.2$ times the mass of the sun $(1.2M_\odot)$, disk inner and outer radii $R_{\mathrm{in}} = 5 \times 10^8$ cm and $R_{\mathrm{out}} = 4 \times 10^{10}$ cm, and mass transfer rate of the companion $\dot{M}_{\mathrm{T}} = 10^{-9}\ M_\odot$ year^{-1}.

The evolution of a disk annulus as it goes into quiescence in a standard model is represented by triangles in Fig. 1. The evolution when physically motivated values of α are used (circles) shows that the disk does not saturate at a low level of MHD turbulence, but suffers a runaway cooling as dissipation and Re_{M} become less and less important.